

MicroCT visualization of the membranous labyrinth

J. Goyens¹

¹University of Antwerp, Laboratory of Functional Morphology, Universiteitsplein 1, 2610 Wilrijk, Belgium

Aims

The membranous labyrinth is crucial for balance during many everyday tasks. It is part of the vestibular system in the inner ear, and it senses head rotations and translations during (for example) locomotion. The vestibular system consists of 3 interconnected tunnels in the skull bone (the bony labyrinth), which are filled with a water-like fluid (perilymph). 3 interconnected ducts with membranous walls float within the perilymph, and constitute the membranous labyrinth. Also the membranous labyrinth is filled with a water-like fluid, called endolymph¹.

The membranous labyrinth is interesting from an evolutionary point of view (given its crucial role in locomotion), but also from a clinical perspective, because of the high prevalence of balance disorders with debilitating effects on patients². Unfortunately, research on the functioning of the membranous labyrinth is hampered by the difficulty of visualizing its membranous walls. Histological sectioning causes large artefacts (as do other methods that require extensive sample preparation, such as light sheet fluorescence microscopy), and it is difficult to acquire sufficient contrast using microCT scanning. The latter is caused by the embedding of the membranous labyrinth in the dense skull bone, the thinness of the membranous (only about 10-15 µm) and the similarity in X-ray density of the membranes and the surrounding liquid³⁻⁵.

These visualization challenges may be overcome by using synchrotron radiation as the source for microCT scanning (rather than a conventional X-ray tube)⁶. However, the access to synchrotron microCT scanners is limited and may be expensive. Therefore, we aimed to find acquisition settings for conventional microCT scanners that also enable sufficient contrast of the membranous labyrinth to enable (at least manual) segmentation of the membranes.

The smaller the specimen, the harder it becomes to visualize the membranous labyrinth. Therefore, we chose lizards as study specimens, whose vestibular systems can be smaller than 1 mm.

Method

Sample preparation A *Takydromus sexlineatus* lizard was purchased from a commercial dealer (Fantasia Reptiles, Antwerp, Belgium), and *Lacerta agilis* and *Phoenicolacerta laevis* specimens from the historical collection of the FunMorph lab. Their heads were fixated in 4% formaldehyde, and subsequently stained in Phosphotungstic acid for 3 weeks.

Skyscan 1172 – scan A In a first attempt to visualize the membranes, we used our standard settings for the visualization of the anatomy of small head specimens in our skyscan 1172 scanner (<https://sites.google.com/view/biostruct>). For an overview of the scanning parameters, see Table 1. This scan took 3h20min and resulted in an image pixel size of 2.49 µm.

Skyscan 1172 – scan B Because the membranes were invisible in scan A, we subsequently adapted our acquisition settings according to David et al.⁷ (see Table 1). These authors successfully visualized the membranous labyrinth of larger specimens using conventional microCT scanning. Scan B took 10h27min and had an image pixel size of 2.49 µm.

Skyscan 1172 – scan C Since the membranes are made of low dense material, high energy X-rays readily pass through this soft tissue without being absorbed⁸. Hence, we tested whether their

contrast could be further improved by reducing the source voltage from 100 kV to 60 kV (see Table 1). However, in order to obtain sufficient X-ray transmission through the sample, we had to increase the exposure time of the camera. Because this elongates the scan, we recorded over 180° instead of 360°, in order to maintain a similar scanning duration.

Skyscan 1272 – scan D Using similar settings as scan C, we performed a scan in the newer Skyscan 1272 machine (see Table 1). In an attempt to obtain the best possible contrast, we increased the rotation range to 360°. We reduced the exposure time by half to compensate for software differences between both scanners.

Table 1: scan parameters

	Scan A	Scan B	Scan C	Scan D
Scanner	Skyscan 1172	Skyscan 1172	Skyscan 1172	Skyscan 1272
Species	<i>P. laevis</i>	<i>L. agilis</i>	<i>T.</i> <i>sexlineatus</i>	<i>T.</i> <i>sexlineatus</i>
Source voltage	100 kV	100 kV	60 kV	60 kV
Source current	100 µA	100 µA	165 µA	165 µA
Exposure time	1.7 s	1.7 s	3.08 s	3.08 s
Frame averaging	4	6	6	3
Rotation step	0.17°	0.15°	0.11°	0.11°
Rotation range	180°	360°	180°	360°
Filter	1 mm Al-Cu	1 mm Al-Cu	1 mm Al	1 mm Al

Results

On the initial, short scan (scan A), the membranes are hardly (or not) visible, even though the scan does not suffer from ring artefacts, movement artefacts or depletion artefacts (see Fig. 1).

Reducing the rotation step, scanning over a 360° range and increasing the frame averaging (scan B, see Fig 2) improves the contrast. The membranes become vaguely visible on some of the reconstructed slices. However, on most slices the membranous labyrinth is still invisible and the signal-to-noise ratio remains low.

Reducing the source voltage has more effect. In scan C (see Fig. 3), the contrast of the membranes is substantially improved, and the noise in the reconstructed slices is reduced. Together, this enables manual segmentation of the membranous labyrinth.

Finally, the 360° scan on the newer 1272 Skyscan machine results in an even better contrast and signal-to-noise ratio (scan D, see Fig. 4).

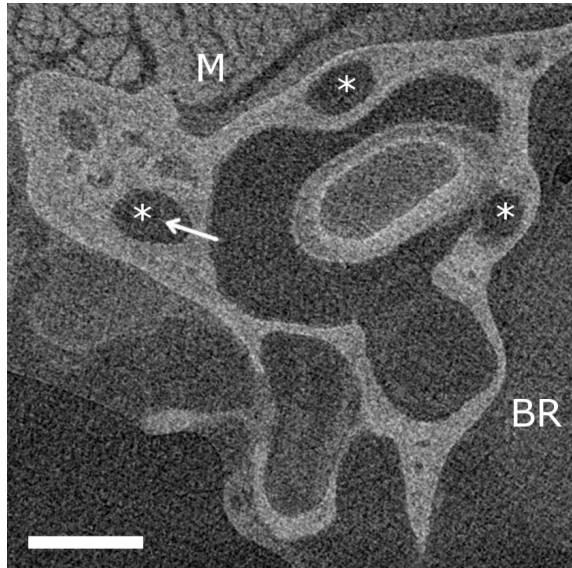


Figure 1: reconstructed slices of *P. laevis* made by a 1172 Skyscan scanner. Ducts of the membranous labyrinth (*), brain tissue (BR) and muscle tissue (M) are indicated. The arrows point to the membranes. The scale bar indicates 0.5mm.

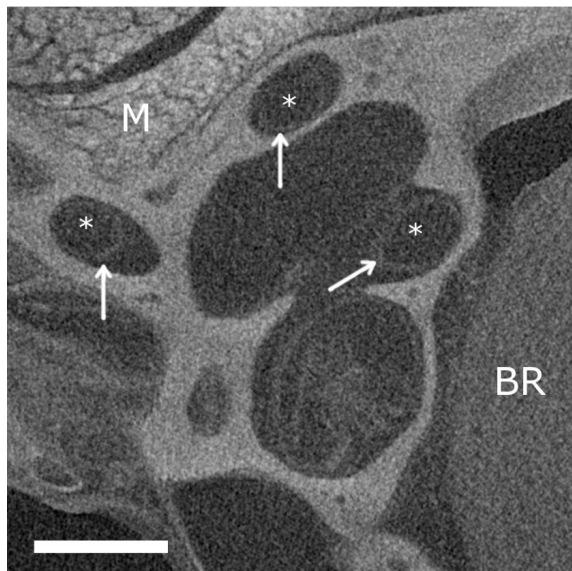


Figure 2: reconstructed slices of *L. agilis* made by a 1172 Skyscan scanner. Ducts of the membranous labyrinth (*), brain tissue (BR) and muscle tissue (M) are indicated. The arrows point to the membranes. The scale bar indicates 0.5mm.

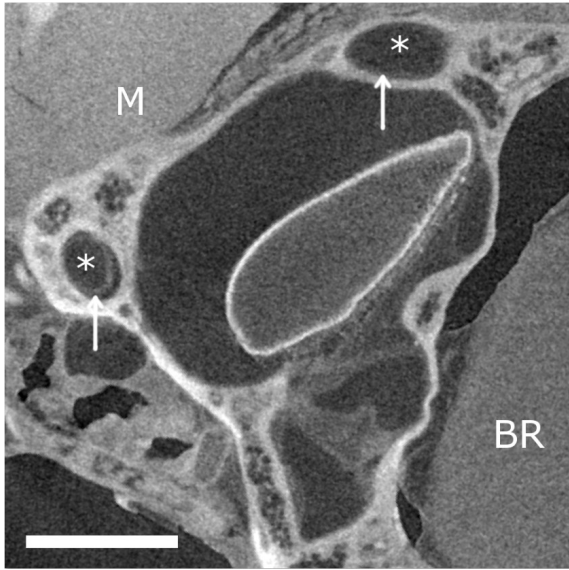


Figure 3: reconstructed slices of *T. sexlineatus* made by a 1172 Skyscan scanner. Ducts of the membranous labyrinth (*), brain tissue (BR) and muscle tissue (M) are indicated. The arrows point to the membranes. The scale bar indicates 0.5mm.

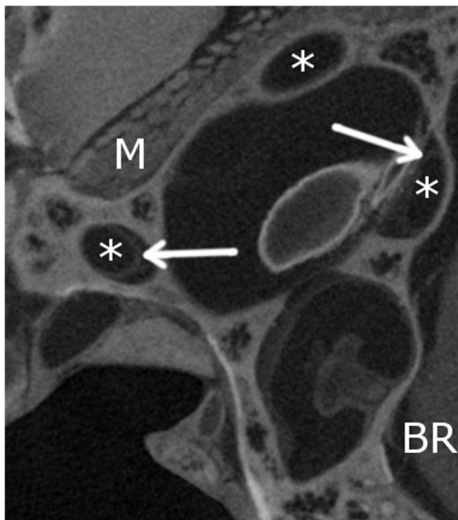


Figure 4: reconstructed slices of *T. sexlineatus* made by a 1272 Skyscan scanner. Ducts of the membranous labyrinth (*), brain tissue (BR) and muscle tissue (M) are indicated. The arrows point to the membranes.

Conclusion

Visualising the membranous labyrinth in the inner ear by microCT is very challenging because its membranes are very thin, and because they consist of soft tissue that is embedded in dense skull bone^{3,9,5}. We found that it is possible to substantially improve the contrast and signal-to-noise ratio by a careful optimisation of the scanning parameters of a microCT system with a conventional X-ray tube. Especially reducing the source voltage proved to be very beneficial. Hence, it is not necessary to rely on synchrotron microCT scanning in order to visualise the membranous labyrinth by computed tomography.

References:

1. Squire, L. R., Berg, D. & Bloom, F. E. "Fundamental neuroscience". (Elsevier/Academic Press, 2013).
2. Agrawal, Y., Carey, J. P., Della Santina, C. C., Schubert, M. C. & Minor, L. B. "Disorders of balance and vestibular function in US adults". *Arch. Intern. Med.* **169**, 938–944 (2009).
3. Wu, C. & Wang, K. "Three-dimensional Models of the Membranous Vestibular Labyrinth in the Guinea Pig Inner Ear". in 4th International Conference on Biomedical Engineering and Informatics 544–547 (2011).
4. Ekdale, E. G. "Form and function of the mammalian inner ear". *J. Anat.* **228**, 324–337 (2016).
5. Curthoys, I. S., Blanks, R. H. & Markham, C. H. "Semicircular canal radii of curvature (R) in cat, guinea pig and man". *J. Morphol.* **151**, 1–15 (1977).
6. Glueckert, R. et al. "Histology and synchrotron radiation-based microtomography of the inner ear in a molecularly confirmed case of CHARGE syndrome". *Am. J. Med. Genet. A* **152A**, 665–73 (2010).
7. David, R., Stoessel, A., Berthoz, A., Spoor, F. & Bennequin, D. "Assessing morphology and function of the semicircular duct system: introducing new in-situ visualization and software toolbox". *Sci. Rep.* **6**, 32772 (2016).
8. Bushberg, J. T., Seibert, J. A., Leidholdt, E. M. & Boone, J. M. "The essential physics of medical imaging". (Lippincott Williams & Wilkins, 2002).
9. Zachary, J. F. & Mc Gavin, M. D. "Pathologic Basis of Veterinary Disease". (2016).